Optics Communications 284 (2011) 651–655

Contents lists available at ScienceDirect

Optics Communications

journal homepage: www.elsevier.com/locate/optcom

Observation of simultaneous reverse saturation absorption and saturation absorption in silver nanoparticles incorporated into europium oxide thin film

F.Z. Henari [a,*], A.A. Dakhel [b]

[a] Royal College of Surgeons in Ireland — Bahrain, P.O. Box 15503, Bahrain
[b] Department of Physics, College of Science, University of Bahrain, P.O. Box 32038, Bahrain

ARTICLE INFO

Article history:
Received 7 April 2010
Received in revised form 9 September 2010
Accepted 9 September 2010

Keywords:
Optical properties
Europium–silver oxide
Ag-incorporated Eu oxide
Oxides
Z-scan
Nonlinear optical properties

ABSTRACT

In this work, nano silver clusters incorporated into europium oxide thin films at a level of 3.8% and 12.5% have been prepared by a vacuum evaporation method on glass and silicon substrates. Samples were investigated by X-ray fluorescence, X-ray diffraction, and linear and nonlinear optical absorption methods. The X-ray diffraction reveals that the Eu oxide of these samples remains amorphous after pre-annealing at 400 °C. The linear optical absorption of the samples shows surface plasmon resonance (SPR) phenomena, which varies with the Ag content of the samples. The optical nonlinear absorption properties of the prepared films were investigated using an open Z-scan technique with cw laser at wavelengths 476 nm and 514 nm. A changeover from reverse saturation absorption (RSA) to saturation absorption (SA) was observed. RSA is attributed to interband transition via two photon absorption. SA is attributed to plasmon bleach.

1. Introduction

It is known that metallic nanoparticles or nanoclusters embedded in an insulating matrix have their particular effects on the optical properties of the matrix like creation of surface plasmon resonance (SPR) and optical nonlinearity due to the quantum size effect (QSE). Thus the optical and optoelectronic properties of a matrix that contains nanoparticles are dependent on their type, sizes and shapes as well as the properties of the matrix itself. Consequently, it is possible to control the physical properties of a matrix by changing these parameters [1]. Such property control is useful in the development of many microelectronic and optoelectronic devices like optical switching and high-speed optical logic devices, as well as other applications like chemical gas sensors, etc. [2–7]. Silver nanoparticles incorporated in an insulating medium have many applications like the intensification of luminescence [8–11] and enhancement of nonlinear optical properties especially the third order nonlinearity [4,6,12]. However, the study of the nonlinear optical properties of silver nanoparticles supported on rare-earth oxides is absent from the literature.

The nonlinear optical properties of metallic nanoparticles have been of great interest due to their potential applications in the optical, medical and biological fields [13]. Several mechanisms contribute to the nonlinear properties of these materials including surface plasmon resonance (SPR), interband transitions between the d-band and conduction band and intraband transitions in the quantum confined conduction band [14]. Gold, cobalt, silver, and nanoclusters in thin films, in colloids and in different glasses are widely studied for nonlinear optical properties and switching applications. Saturation absorption (SA), reverse saturation and absorption (RSA) of these materials have been reported [15,16] and are possibly utilized for Q-switching and optical power limiting respectively. Recently simultaneous influence of saturation and reverse saturation was reported in copper and gold particles [17,18]. Yachen Gao et al. [19] reported a shift from saturation absorption in Pt nanoparticles at a wavelength of 532 nm and found that the sample shows saturable absorption at low intensities and reverse saturable absorption at higher intensities. K. P. Unnikrishnan et al. [20] investigated the nonlinear absorption in silver nanosol at selective wavelengths. They observed that the change over between saturable absorption and reverse saturable absorption is sensitive to the intensity as well as the excitation wavelength. R. A. Ganeev et al. [21] studied the optical nonlinearity of copper nanoparticle embedded in silicon glass at the laser wavelength (532 nm, pulse width 5 ns) close to the SPR peak. They also observed the simultaneous change over from reverse saturation absorption to saturation absorption. It was shown that with an increase in intensity the saturation absorption becomes dominant in comparison with reverse saturation absorption. Shiliang Qu et al. [14] investigated the nonlinear absorption of Au and Ag nanoparticles precipitated in the glasses by using Z-scan with nanosecond pulses at 532 nm. They observed the saturable absorption behaviour for Au nanoparticles and reverse saturable behaviour for Ag nanoparticles. F. Henari et al. [22] reported the nonlinear absorption of Au nanoparticles incorporated onto europium oxide film using Z-scan

* Corresponding author. Tel.: +973 17 351450; fax: +973 17 330806.
E-mail addresses: fzhenari@rcsi-mub.com (F.Z. Henari), adakhil@sci.uob.bh (A.A. Dakhel).

0030-4018/$ – see front matter © 2010 Elsevier B.V. All rights reserved.
doi:10.1016/j.optcom.2010.09.090

with continuous wave at 633 nm. They observed the saturable absorption behaviour for Au nanoparticles at a considerable low power.

In this paper, we conduct investigation on the Ag nanoparticles incorporated on europium oxide film using the Z-scan technique. The Z-scan experiment was performed with cw argon laser at wavelengths 476 nm and 514 nm at different laser power ranging between 14 and 40 mW. Although the reverse saturation absorption of the Ag has been reported using pulsed lasers. Our study demonstrates the observation of simultaneous reverse saturation absorption and saturation absorption at wavelengths of the vicinity of the SPR peak with cw laser beam.

2. Experimental details

The starting materials were a pure europium element (from Fluka A. G.) and pure silver metal (from Aldrich chem. Co). The alternating thermal deposition (layer-by-layer, etc) method was used to deposit the starting materials on ultrasonically clean glass and clean silicon wafer substrates held at about 150 °C in a vacuum chamber of residual oxygen atmosphere of pressure about 1.3×10^{-2} Pa. The evaporated mass and thickness were controlled with a Philips FTM 5 thickness monitor. Two groups of samples of different Ag content (S1 and S2) were prepared in the present study. For stabilisation of the as-grown films, the samples were held in oxygen atmosphere at 150 °C for about 20 h. The final film thicknesses were measured by Gaertner L117 ellipsometer and found to be 0.15–0.20 m. The as-prepared samples were then pre-annealed at temperature 400 °C for 6 h. The structure of the prepared films was studied by the X-ray diffraction (XRD) method using a Philips PW1710 – 2 system. The study of the elemental content and the measure of the molar content of Ag relative to Eu (r) were performed by an energy dispersion X-ray fluorescence (EDXRF) technique with Cu K_α exciting radiation and an Amptek XR-100CR detector. The spectral optical transmittance $T(\lambda)$ was measured at normal incidence in UV–VIS spectral region (190–1000 nm) with a Shimadzu UV-3600 double beam spectrophotometer. The procedure was carried out firstly by preparing a group of samples with small r (S1), which was measured to be about 2.5 wt.%, and other samples (S2) with more Ag content of about 8.9 wt.% were prepared. The nonlinear absorption properties of the sample S2 were studied by using a standard far-field Z-scan technique [23]. The Z-scan experiment was performed with a continuous wave (cw) visible argon ion laser at wavelengths 476 nm and 514 nm with an average power of 40 mW. The beam was focused to a beam waist of 20 μm with a lens of 5 cm focal length, giving a typical power density of 6×10^7 W/m^2. The nonlinear absorption experiment was performed only on the S2 sample because it contains corporeal Ag-nanograins as observed in Fig. 2.

3. Characterisation by X-rays

Fig. 1 shows the EDXRF spectrum of the studied Ag-incorporated Eu-oxide films on the Si substrate samples. It shows that there is no other signal except the signals of the elements in the films Eu L-spectrum (L_α, L_β, and L_γ), Ag L-band, as well as signals from the exciting source and the silicon substrate. The relative molar fraction ratio (r) of Ag to Eu in the prepared films was determined by the well-known method of XRF micro radiographic analysis [24]. It is based on measuring the integral intensity ratio of Eu L (5.84 keV) line and Ag L (2.98–3.34 keV) band in reference samples and film samples. The reference samples were pure thin Eu_2O_3 and Ag films. The result of calculation of r was about 3.8 molar% for S1 and 12.5 molar% for S2.

The structure of the prepared Ag-incorporated Eu-oxide films was investigated by the method of XRD and the results are shown in Fig. 2. The observed hump around 21° corresponds to the glass substrate. The pattern reveals that Eu oxide does not crystallise under annealing at 400 °C for both S1 and S2. The absence of any X-ray reflection from Ag reveals that it was not crystallised; it aggregated as clusters within the Eu-oxide amorphous medium, the hump around $2\theta = 32°$.

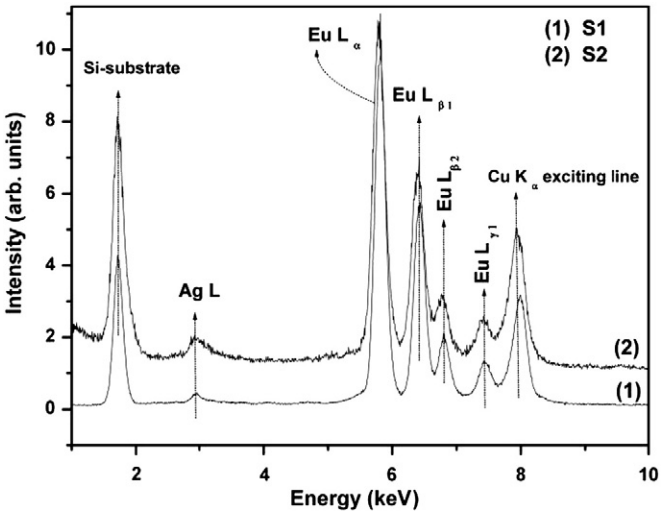

Fig. 1. The EDXRF spectrum of S1 and S2 Ag-incorporated Eu-oxide films grown on the Si substrate. The exciting radiation was Cu K of energy 8.047 keV.

4. Linear optical properties

The spectral absorbance in the wavelength range (200–1000 nm) was measured and the results are shown in Fig. 3. It shows clear SPR bands in both films at wavelength 410 nm for S1 and 460 nm for S2. Such peaks do not exist in the spectrum of pure polycrystalline Ag film nor in the pure Eu-oxide film.

These SPR absorption peaks are attributed to the formation of metal nanoclusters in the amorphous Eu-oxide medium, which have a different optical response (due to their small sizes) than the surrounding medium [4,7,25,26]. It is possible to estimate the average size of the Ag nanoclusters by using the classical Mie theory [4]: $r_{Mie} = v_F/\Delta\omega_{1/2}$, where r_{Mie} is the Mie average radius of metal spheres, v_F is the Fermi velocity (1.39×10^6 m/s for Ag) and $\Delta\omega_{1/2}$ is the full width at half maximum (FWHM) in the angular frequency scale, of the absorption SPR peak. This relation supposed that the light-scattering particles are spherical and there is no interparticle coupling. Therefore, it gives very small values for r_{Mie}. The experimental FWHM $\Delta\omega_{1/2}$values must reflect the effect of nanoparticle size in addition to the interparticle coupling and it is a good practical parameter that we will use as $\Gamma = 1/\Delta\omega_{1/2}$, which is proportional to the effective nanoparticle radius. The experimental values of Γ are: 7.37×10^{-16} s and 6.13×10^{-16} s for S1 and S2,

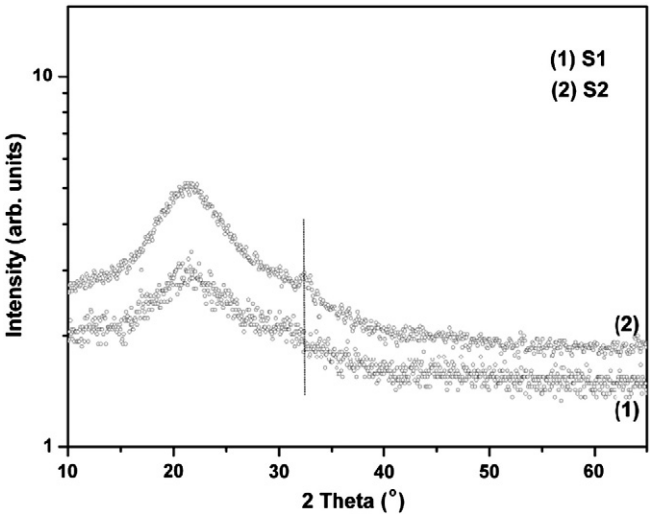

Fig. 2. The XRD patterns of Ag-incorporated Eu oxide S1 and S2 films grown on the glass substrate. The radiation used was Cu K-line of wavelength 0.1543 nm.

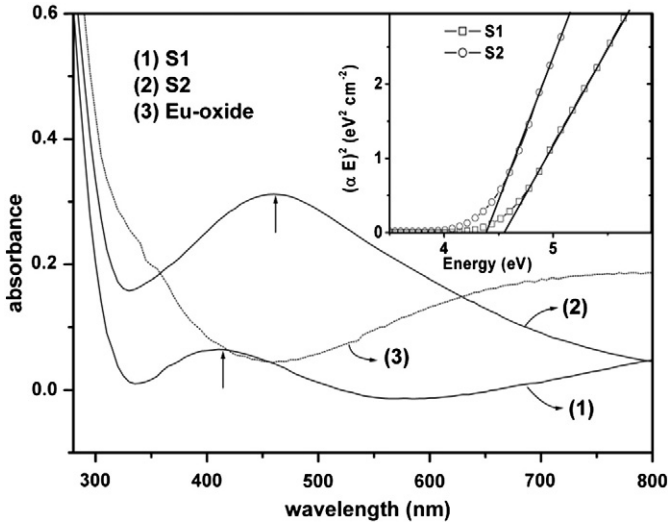

Fig. 3. Absorption spectra of pure Eu_2O_3 and Ag-incorporated Eu oxide S1 and S2 films grown on the glass substrate. The inset shows the relationship $(\alpha E)^2$ vs. E for S1 and S2 samples.

respectively. Thus, for both samples $r_{Mie} \sim 10\ nm$, the energy position of the SPR peaks depends on the type and state of the medium around the Ag nanoparticles in addition to the physical properties of the nanoparticles and the interparticle dipole–dipole interaction. In the present work, it was observed that the SPR peak is red shifted by increasing the Ag content in the Eu-oxide matrix. This observation is supported by ref. [27] that the increase of %Ag content leads to the decrease of the average distance between the nanoparticles, which red shifts the SPR peak due to the interparticle coupling effect on SPR; similar observation was observed in ref. [28] to Ag nanoparticles in a colloidal solution. Furthermore, it is observed in the present work that increasing of the Ag content enhances the peak height, enhancement of *FWHM* in wavelength scale $\Delta\lambda_{1/2}$(121 nm for S1 to 183 nm for S2) in addition to the red shift of λ_p. The peak enhancement can be explained due to the increased volume fraction of the metal colloids resulting from greater segregation of the metal Ag particles in the Eu-oxide medium.

The spectral linear absorption coefficient $\alpha(\lambda)$was calculated approximately by $\alpha_o = (1/d)\ln(1/T)$, where d is the film thickness. The experimental data of the transmittance T were taken relative to the identical clean glass substrate. The optical bandgap E_g is evaluated according to the well-known relation [29,30]:

$$\alpha_o = A\left(E - E_g\right)^m \tag{1}$$

where A is a constant and the exponent m is equal to 0.5 or 2 for direct and indirect transitions, respectively. It is observed that the best value suitable to the data of the present work is $m = 0.5$. Therefore, the plot of $(\alpha_o E)^2$ vs. E, as shown in the inset of Fig. 3. It gives the values of direct bandgaps 4.54 eV and 4.38 eV for S1 and S2, respectively. For both cases E_g is larger than that of pure Eu_2O_3, which is 4.25 eV, as measured by us using the same method. Thus doping of Eu_2O_3 with Ag leads to increasing E_g by about 0.15 eV and also E_g increased with increasing Ag content to 0.25 eV.

5. Open aperture Z-scan

The nonlinear absorption of the sample S2 was investigated using the well-known open aperture Z-scan technique [23]. This technique relies on the fact that the intensity varies along the axis of the convex lens and it is maximum at the focus. Hence, by shifting the sample through the focus, the intensity dependence can be measured as a change in transmission. The transmission from the sample was measured without an aperture (open Z-scan) in the far field. The open Z-scan experiment was performed with an argon ion laser at two different wavelengths (476 nm and 514 nm). The laser beam is focused onto the sample using a lens of 5 cm focal length to a beam waist of 20 μm, yielding a typical power density ranging from 1.12×10^7 W/m^2 to $3.18.1\times10^7$ W/m^2 for different input intensities. The sample is moved across the focus by a translation stage driven by a stepping motor. The transmission output from the sample is collected by a lens and focused to a detector, which is connected to the data acquisition system. Due to the inherited inhomogeneity during film preparation, all necessary steps were taken to make sure that both the X-ray and Z-scan experiments were performed at the same point of the film.

Fig. 4 shows the normalized transmittance without an aperture as a function of the distance along the lens axis z, for a 0.255 μm thick sample (S2) at wavelength away from the SPR peak (=514 nm). The transmission is symmetric with respect to the focus ($z=0$), where it has a minimum transmission. This demonstrates that the sample exhibits RSA (optical limiting). This effect has been observed for Ag nanoparticles [14,20] as well as for platinum [19]. The open Z-scan was performed at different incident intensities. As the incident intensity is increased, the transmission change ΔT decreases from 0.23 to 0.18. This reduction of the ΔT is believed to be due to the influence of the saturation absorption processes. This behaviour allows us to believe that the existence of both SA and RSA are present in the sample. However, the intensity of the laser was not enough to see change over from RSA to SA at this particular wavelength. For the case when only RSA is present, the normalized transmission for the open Z-scan is given by [23].

$$T = 1 - \left(\frac{1}{2\sqrt{2}}\frac{\alpha I_o L}{(1+x^2)}\right) \tag{2}$$

where $x = z/z_0$ (with $z_0 = w_o^2/\lambda$) z_o is the diffraction length of the Gaussian beam and w_o is the beam's waist radius, and $L = (1-\exp(-\alpha_o d))/\alpha_o$ with α_o is a linear absorption coefficient and d is the sample thickness, L is the effective thickness of the sample. I_o is the intensity of the laser beam at the focus and is the total nonlinear absorption. For the open case when only RSA is present (=). The fit of Eq. (2) to the Z-scan data is shown in Fig. 4 and yields the values of the nonlinear absorption coefficient $=2.5\times10^{-3}$ m/W, $=1.5\times10^{-3}$ m/W for intensities 1.12×10^7 W/m^2 and 3.18×10^7 W/m^2 respectively at wavelength 514 nm. The reduced value of is an indicative of the existence of both SA and RSA processes. The Z-scan was performed in a pure Eu-oxide film, where no nonlinear response was observed at the intensities used in the experiment.

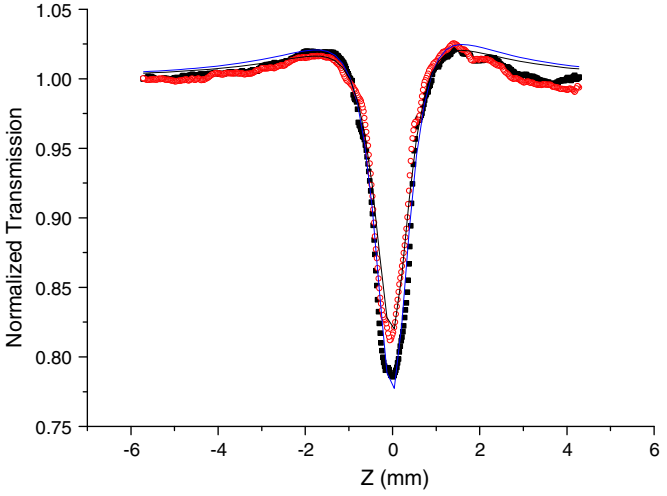

Fig. 4. Open aperture Z-scan response for intensities 1.12×10^7 W/m^2 (squares) and 3.18×10^7 W/m^2 (circles); the points represent the measuring data; the lines corresponds to the fit Eq. (2).

Fig. 5 shows the normalized transmittance without an aperture as a function of the distance along the lens axis z, for the sample S2 at a wavelength close to SPR (=476 nm). The sample shows RSA properties because of a minimum transmission at the focus ($z=0$). The initial weak increase in transmission may be due to a weak contribution of the nonlinear refractive index following by strong nonlinear absorption. As the intensity of incident beam increased, the negative peak (i.e. ΔT) is decreasing from 0.35 to 0.25. Further increase in the intensity results in the appearance of the SA peak Fig. 5a. Additional increase in the intensity leads to an increase in the size of the SA peak as shown in Fig. 5b. This behaviour allows us to conclude that the RSA and SA are simultaneously present in the sample and better defined at the wavelengths close to the SPR peak.

For the case, when both RSA and SA are present in the sample. The total nonlinear absorption coefficient is given by

$$\alpha(I) = \frac{\alpha_o}{1 + \frac{I}{I_s}} + I\beta \tag{3}$$

When the first term describes SA, and the second term describes RSA. α_o is the absorption coefficient of the sample, I and I_s are laser radiation intensity and saturation intensity respectively. is the nonlinear absorption coefficient. Combining Eqs. 1 and 2 results in

$$T = 1 - \left[\frac{1}{2\sqrt{2}}\left[\frac{\alpha_o I_o L}{(1 + I/I_s)(1 + x^2)} + \frac{\beta I I_o L}{(1 + x^2)}\right]\right]. \tag{4}$$

The fit of Eq. (4) to the Z-scan data is shown in Fig. 5. The experimentally determined value of I_s and for the sample at different incident intensities was found to be, $I_s = 1.7\times10^6$ W/m^2, $=3.68\times10^{-4}$ m/W, $I_s = 3.18\times10^6$ W/m^2 and $=1.2\times10^{-4}$ m/W.

Fig. 6 shows a plot of the normalized transmission dependence for the sample, which was calculated using Eq. (3) with different incident intensities values ranging from 1×10^7 W/m^2 to 6×10^7 W/m^2. Other parameters such as $_o$ and I are kept constant. The plot is in agreement with the observed experimental results. The range of values of and I_s are displayed in Fig. 6. The values of and I_s have pronounced effects on the change over from reverse saturation absorption to saturation absorption. RSA is dominated at a higher value of while, SA is dominated at higher values of I_s (inset).

The processes leading to the observed nonlinear properties of Ag nanoparticles are under intensive studies [31–33]. A simple three level system model was considered to explain reverse saturation absorption and saturation absorption behaviours [18,20]. The model takes into account the surface plasmon absorption, free carrier absorption and two photon absorption. The same model can be applied to explain our results. The RSA of Ag films arises from the interband transition from 4d to 5 s states via two photon absorption. The excitation wavelengths used in the experiment were 514 nm and 476 nm corresponding to the photon energies 2.3 and 2.6 eV respectively, which are smaller than the bandgap energy 4.38 eV measured above. In this case, the only possible transition would be through a two photon absorption that leads to direct pumping of electrons to the plasmon state. However, the electrons in the plasmon band are free carriers with a whole spectrum of energy. When the excitation wavelength is close to the SPR wavelength and the intensity is high, the electrons from the ground state plasmon band are excited. This results in frequency differences between the excited electrons and the remaining unexcited electrons in the SPR band. Therefore, the electrons in the original SPR band cannot further absorb radiation. This results in SA behaviour (SPR bleach). The thermal effect also contributes to a nonlinear effect and may arise from the use of cw laser beam which leads to thermalizing of hot electrons and subsequent dissipation of their energy leads to increase in the surrounding

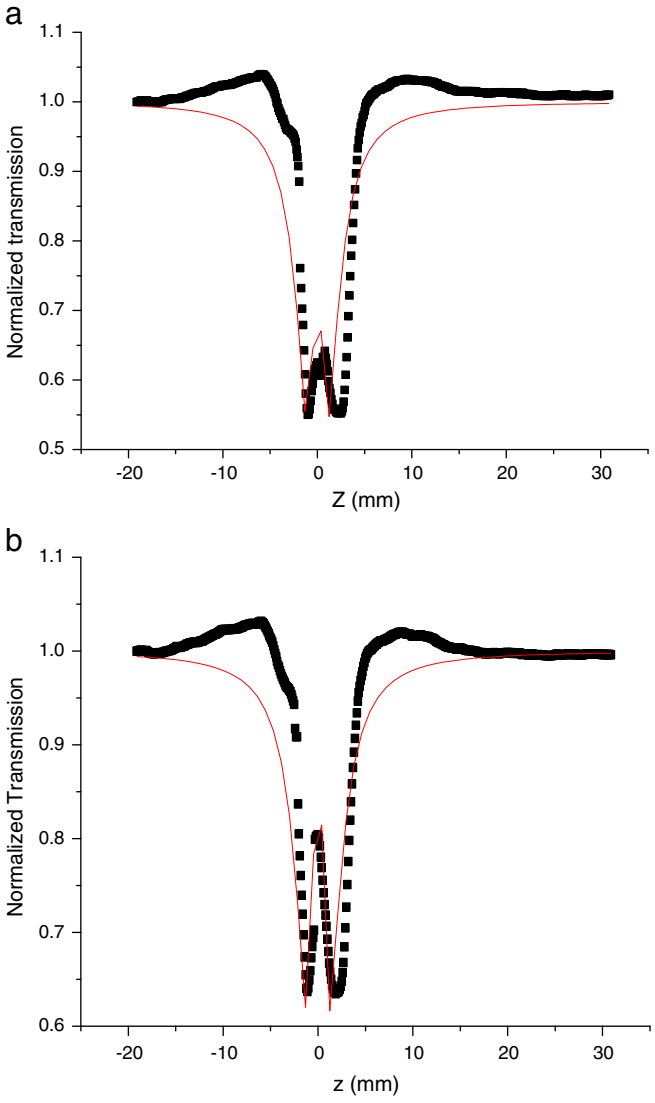

Fig. 5. Open aperture Z-scan response; the points represent the measuring data; the line corresponds to the fit Eq. (4). a — at incident intensity 1.1×10^7 W/m^2. b — at intensity 3.2×10^7 W/m^2.

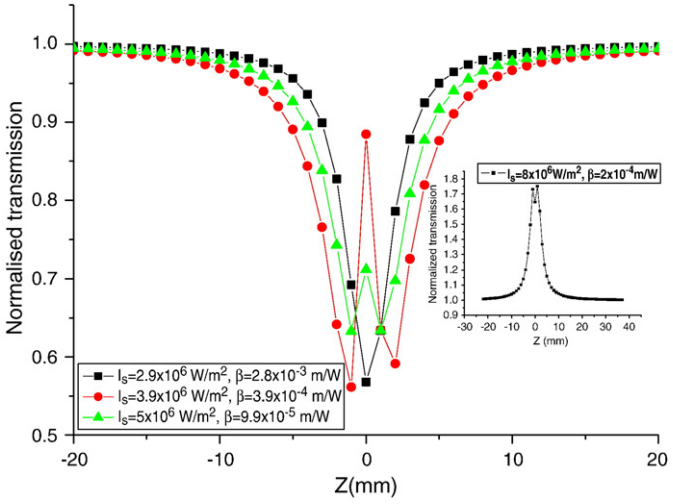

Fig. 6. Normalized transmission dependence on Z for the sample S2, calculated using Eq. (4) with different incident intensities values ranging from 1×10^7 W/m^2 to 6×10^7 W/m^2.

temperature which results in variation of refractive index change and through Kramers–Kronig relation to change in absorption.

According to the above analysis and our experimental results, we conclude that the nonlinear absorption response arises from inter-band transition via two photon absorption results in RSA and intraband transition for SA behaviour as a result of a bleach ground state plasmon band. However detailed studies must be performed in order to determine the exact origin of the change over from RSA to SA.

6. Conclusions

X-ray diffraction patterns show that the prepared Ag-incorporated Eu-oxide samples pre-annealed at 400 °C are amorphous and Ag does not crystallise. The optical absorption spectrum shows that Ag nanoparticles or nanoclusters exhibit surface plasmon resonance (SPR) band due to quantum size effect (QSE). Ag nanoparticles' Mie radius was estimated to be about 1 nm. It was observed that the SPR peak position is red shifted by increasing of the Ag content in the Eu-oxide matrix. These observations were explained according to the available models and previous works. The nonlinear absorption of Ag-incorporated Eu-oxide samples was studied at two different wavelengths. The sample can act as a RSA absorber and a SA absorber at the same wavelength depending on the input intensity. The results were explained in view of the interband transition via two photon absorption for RSA behaviour and SPR band bleach for RSA behaviour. The change over from RSA to SA will provide the basis for optical switching and gating devices. An extensive investigation of the origin of the nonlinear absorption is needed before the use of these materials in devices.

References

[1] A.P. Alivisatos, Science 271 (1996) 933.
[2] J.W.M. Chon, C. Bullen, P. Zijlstra, M. Gu, Adv. Funct. Mater. 17 (2007) 875.
[3] M. Menning, M. Schmitt, U. Becker, G. Jung, H. Schmidt, Proceedings of SPIE, Sol–Gel Optics III, vol. 2288, 1994, p. 130.
[4] B. Ghosh, P. Chakraborty, S. Mohapatra, P.A. Kurian, C. Vijayan, P.C. Deshmukh, P. Mazzoldi, Mater. Lett. 61 (2007) 4512.
[5] D. Kundu, I. Honma, T. Osawa, H. Komiyama, J. Am. Ceram. Soc. 77 (1994) 1110.
[6] S. Ogawa, Y. Hayashi, N. Kobayashi, T. Tokizaki, A. Nakamura, Jpn. J. Appl. Phys. 33 (1994) L331.
[7] G. Teowee, K.C. McCarthy, T.J. Bukowski, T.P. Alexander, S. Motakef, D.R. Uhlmann, Proc. Tenth. IEEE International Symposium on Applications of Ferroelectrics ISAF, vol. 2, 1996, p. 671.
[8] J.A. Jiménez, S. Lysenko, H. Liu, J. Luminescence 128 (2008) 831.
[9] B. Lipowska, A.M. Klonkowski, J. NonCryst. Solids (2008), doi:10.1016/j.jnoncrysol.2008.06.055.
[10] Y. Wang, X. Zhou, T. Wang, J. Zhou, Mater. Lett. 62 (2008) 3582.
[11] Y. Wang, J. Zhou, T. Wang, Mater. Lett. 62 (2008) 1937.
[12] T. Jia, T. He, P. Li, Y. Mo, Y. Cui, Opt. Laser Technol. 40 (2008) 936.
[13] G. Ma, W. Sun, S.H. Tang, H. Zhang, Z. Shen, S. Qian, Opt. Lett. 27 (2002) 1034.
[14] S. Qu, Y. Zhang, H. Li, J. Qiu, C. Zhu, Opt. Mater. 28 (2006) 259.
[15] H.I. Elim, J. Yang, J.Y. lee, J. mi, W. Ji, Appl. Phys. Lett. 88 (2006) 83107.
[16] Q.Q. Wang, J.B. Han, h.M. Gong, D.J. Chen, X.J. Zhao, J.Y. Feng, J.J. Ren, Adv. Funct. Mater. 2405 (2006).
[17] Y. Takeda, j. Lu, O.A. Plaksin, K. Kono, H. Amekura, N. Kishimoto, Thin Solid Films 464–675 (2004) 483.
[18] N. Venkatram, R.S.S. Kumar, D.N. Rao, S.K. Medda, S. De, G. De, J. Nanosci. Nanotechnol. 6 (2006) 1990.
[19] Y. Gao, X. Zhang, Y. Li, H. Liu, Y. Wang, Q. Chang, W. Jiao, Y. Song, Opt. Comm. 251 (2005) 429.
[20] K.P. Unnikrishnan, V.P.N. Nampoori, V. Ramakrishnan, M. Umadevi, C.P.G. Vallabhan, J. Phys. D Appl. Phys. 36 (2003) 1242.
[21] R.A. Ganeev, A.i. Ryasnyansky, A.L. Stepanov, T. Usmanov, Phys . Stat. Sol Rapid research notes 241 (2004) R1.
[22] F.Z. Henari, A.A. Dakhel, J. Of Appl. Phys. 104 (2008) 33110.
[23] M. Sheik- Bahae, A.A. Said, T.H. Wei, D.J. Hagan, E.W. Van Stryland, IEEE J. Quntum Electron. 26 (1990) 760.
[24] J.M. Jaklevic, F.S. Goulding, H.K. Herglotz, L.S. Birks, Energy Dispersion in X-ray Spectrometry, Dekker, NY, 1978, p. 50.
[25] S. Ju, V.L. Nguyen, P.R. Watekar, B.H. Kim, C. Jeong, S. Boo, W.T. Han, J. Nanosci. Nanotechnol. 6 (2006) 3555.
[26] P.R. Watekar, S. Ju, W.T. Han, Colloids Surf. A Physicochem. Eng. Aspects 313/314 (2008) 492.
[27] K.H. Su, Q.H. Wei, X. Zhang, J.J. Mock, D.R. Smith, S. Schultz, Nano Lett. 3 (2003) 1087.
[28] B.H. Choi, H.H. Lee, S. Jin, S. Chun, S.H. Kim, Nanotechnol. 18 (2007) 075706.
[29] J. Tauc, in: F. abeles (Ed.), Optical Properties of Solids, Edited by. North Holland, 1969.
[30] E.A. Davis, N.F. Mott, Philos. Mag. 22 (1970) 903.
[31] A. Kazmin, J. Purans, G. Moreau, J. Alloy. Comp. 374 (2004) 89.
[32] G. Battaglin, P. Calvelli, E. Cattaruzza, R. Polloni, E. Borsella, T. Cesca, F. Gonella, P. Mazzoldi, J. Opt. Soc. Am. B17 (2000) 213.
[33] T.S. Ahmadi, S.L. Wang, M.A. El-Sayed, J. Chem. Phys. 111 (1999) 1255.